Cement and Concrete Research 40 (2010) 1419–1428

Contents lists available at ScienceDirect

Cement and Concrete Research

journal homepage: http://ees.elsevier.com/CEMCON/default.asp

Interaction between corrosion crack width and steel loss in RC beams corroded under load

Goitseone Malumbela *, Mark Alexander, Pilate Moyo

Dpt. of Civil Eng., Univ. of Cape Town, Private Bag X3, Rondebosch, 7700, South Africa

ARTICLE INFO

Article history:
Received 8 October 2008
Accepted 15 March 2010

Keywords:
Concrete (E)
Corrosion (C)
Crack Detection (B)
Service life

ABSTRACT

This paper presents results and discussions on an experimental study conducted to relate the rate of widening of corrosion cracks with the pattern of corrosion cracks as well as the level of steel corrosion for RC beams (153×254×3000 mm) that were corroded whilst subjected to varying levels of sustained loads. Steel corrosion was limited to the tensile reinforcement and to a length of 700 mm at the centre of the beams. The rate of widening of corrosion cracks as well as strains on uncracked faces of RC beams was constantly monitored during the corrosion process, along the corrosion region and along other potential cracking faces of beams using a demec gauge. The distribution of the gravimetric mass loss of steel along the corrosion region was measured at the end of the corrosion process. The results obtained showed that: the rate of widening of each corrosion crack is dependent on the overall pattern of the cracks whilst the rate of corrosion is independent of the pattern of corrosion cracks. A mass loss of steel of 1% was found to induce a corrosion crack width of about 0.04 mm.

1. Introduction

Corrosion of steel bars that are embedded in concrete is the principal cause of deterioration of reinforced concrete (RC) structures that are within the marine environment [1]. It reduces the structural integrity of concrete by the loss in the area of steel, cracking of the cover concrete as well as the loss in the bond between the corroding steel and the surrounding concrete. This is because in addition to reducing the area of steel, corrosion products occupy a larger volume than the parent metal so that their continued production applies tensile stresses on the surrounding concrete, which eventually causes cracking of the cover concrete [1–30].

For those responsible for monitoring the service life of corrosion-affected RC structures such as structural engineers and asset managers, it is important that they identify their easy-to-measure properties that can be directly related to the loss in the area of steel and eventually, the residual capacity of the structures [2,3]. In an attempt to identify these easy-to-measure properties, numerous experimental studies on the behaviour of RC structures with corroding steel bars have been carried out [1–30]. Numerical as well as analytical models such as; the bond between the corroding steel and the surrounding concrete [2,4,5]; the crack width [6–8]; deflections [9]; and ultimate moment capacity of corroded beams [10], have also been developed to predict the behaviour of concrete structures experiencing steel corrosion. These models were, in most cases, calibrated with experimental results that were obtained from RC specimens that were corroded in the absence of a sustained load. Previous studies on steel corrosion of RC structures that were corroded under load [11–16] have, however, revealed that whilst RC structures that were corroded in the absence of a sustained load have been shown to exhibit a gain in the flexural stiffness during the early corrosion stages [17,18], there is never a gain in the flexural stiffness of structures that are corroded whilst under a sustained load. Works by [15,16] showed that after a certain level of steel corrosion on RC beams that were corroded under a constant sustained load, the stiffness of the beams reduced from their near-gross stiffness to their fully-cracked stiffness. The reduced stiffness then remained constant despite a continued increase in the level of corrosion.

Contrasting results were found on the effects of a sustained load on the rate of corrosion. For example, [12,14] reported a larger rate of corrosion for RC beams that were corroded whilst under a constant sustained load compared to RC beams that were corroded in the absence of a sustained load. In contrast, a study by [13] revealed the same level of steel loss for RC beams that were corroded under a sustained load in comparison to RC beams that were corroded in the absence of a sustained load. A review by [11] has therefore recommended that further research needs to be conducted to enable a better understanding of the effects of loading on the rate of corrosion.

Another important finding on the effects of sustained load on corroding RC beams was that it yielded wider corrosion cracks compared to beams that were corroded in the absence of a sustained load [12,13]. A meticulous measurement of corrosion crack widths

* Corresponding author. Tel.: +267 355 4332; fax: +267 395 2309.
E-mail address: malumbela@mopipi.ub.bw (G. Malumbela).

0008-8846/$ – see front matter © 2010 Elsevier Ltd. All rights reserved.
doi:10.1016/j.cemconres.2010.03.010

reported by the researchers was, however, carried out at the end of the corrosion tests when the specimens were removed from their respective loading systems. This was probably because the loading systems used by the researchers did not allow for an easy continuous monitoring of the crack widths during the corrosion process as reported by [11,12]. The sequence and propagation of the cracks with an increase in the level of corrosion was as such unknown. It is however, worth noting that studies by [13] monitored the widening of corrosion crack widths with the level of steel corrosion on beams that were corroded under load. They found corrosion crack widths to generally widen with an increase in the level of corrosion but at a larger rate for beams that were corroded under a sustained load compared to beams that were corroded in the absence of a sustained load. The rate of widening of the crack widths exhibited two distinct stages namely; an initial constant rate of crack widening followed by a reduced but also constant rate of crack widening. The major limitation of the work from [13] is that they took crack measurements at a single point on the beam (centre of the extreme tensile face of the beam) so that the variation of the crack widths along the corroded beam as well as the reasons for a change in the rate of widening of corrosion crack widths was unclear.

Studies by [19] on the lateral deformation of RC beams under simultaneous load and steel corrosion have shown that corrosion crack widths vary along the corrosion region with the largest crack widths experienced at the centre of the region. This indicates that in order to relate corrosion crack widths with the level of steel corrosion, as previously attempted by other researchers [3,6,7,13,20], a full understanding of the variation of both the loss in the area of steel and the crack widths with the level of corrosion as well as along the corroded specimen is necessary. Works by [19] were however, mainly intended to show that lateral deformation of cover concrete due to steel corrosion cannot be modelled by assuming uniform expansion of the cover concrete, which is the basis for models of concrete cover cracking that use the thick-walled cylinder approach [7,21]. In addition, very little work has been done on the variation of loss of steel along corroded specimens, especially when corrosion occurs whilst the specimens are under a sustained load. This is probably because the majority of previous works (even on structures that were corroded in the absence of a sustained load) reported average gravimetric mass loss of steel instead of mass loss of steel at a point along the beam [10,12,13,18,20,22,23].

This paper attempts to fill the aforementioned gaps by providing a further discussion as well as additional results to those that were presented in a previous publication by [19] on the sequence and the rate of corrosion crack widening on RC beams due to steel corrosion. The paper also tries to relate the variation of corrosion crack widths along the beam with the corresponding variation of the level of steel loss. The relation between the variation of the level of steel corrosion and the residual capacity of corroded beams will be published elsewhere.

2. Experimental programme

The experimental programme involved testing eleven quasi-full-scale RC beams ($153\times254\times3000$ mm) under four different levels of sustained loads: 0%, 1% (low deflections), 8% (high deflections but no flexural cracks) and 12% (high deflections and flexural cracks) of the ultimate load capacity of a virgin beam. The detailed loading systems that were used during the corrosion process are discussed in [11,15,19] and are shown in Figs. 1 and 2.

2.1. Reinforcement configuration

Each beam was reinforced with three 12 mm deformed bars in tension and two 8 mm plain bars in compression. The shear reinforcement consisted of 8 mm plain bars spaced at 100 mm (centre-to-centre) in the shear span. No stirrups were placed in the middle span; instead compression reinforcement bars in the middle span were tied together by 8 mm diameter hooks at 200 mm spacing to prevent buckling of compression bars when testing the beams to failure. The reinforcement configuration of the beams is shown in Fig. 3.

2.2. Material properties

All beams were cast using concrete with the same mix proportions with 28 days target strength of 35 MPa. Maximum aggregate size of the concrete was 13.2 mm and w/c ratio was 0.63. Cement, fine sand and coarse aggregate contents were 300 kg, 909 kg and 950 kg/m^3 respectively. Due to the limited number of loading frames to test beams under a sustained load, it was not possible to test beams at the same age. The compressive strength of each concrete was therefore determined at the time of testing using three 100 mm cubes. The

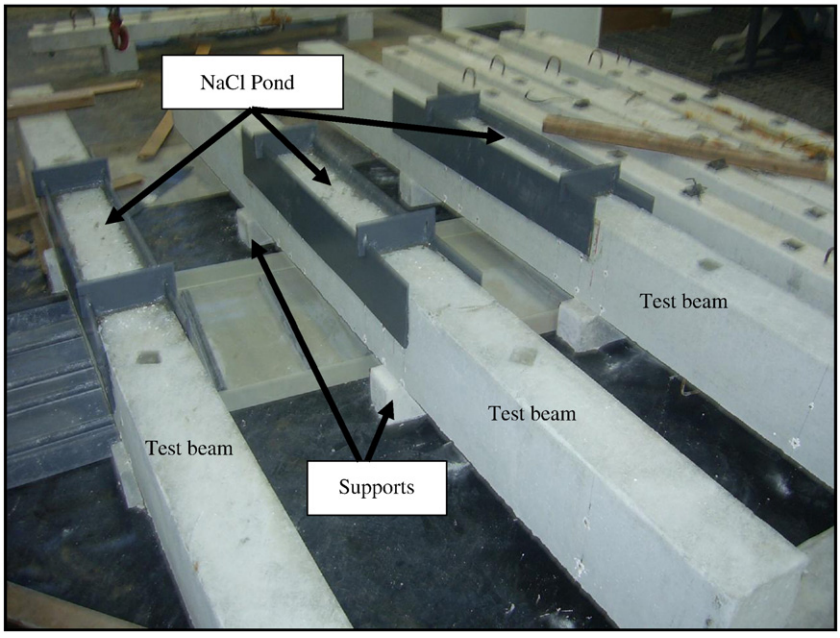

Fig. 1. Test set-up for beams under 1% loading.

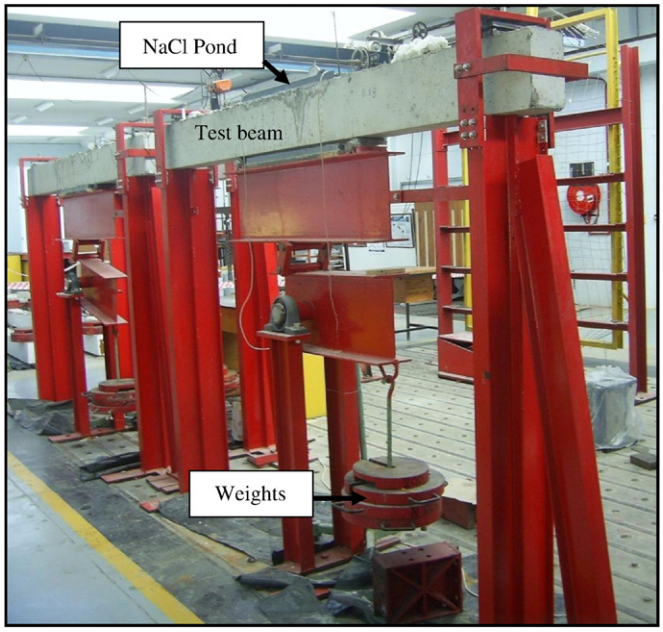

Fig. 2. Test frame for beams under 8% and 12% loading.

measured strength ranged from a minimum of 35.2 MPa (s.d. = 0.8) to a maximum of 50.8 MPa (s.d. = 0.6) as shown in Table 1. Tensile pull tests were carried out on the reinforcing steel bars used in the programme. The 12 mm deformed bars had yield strength of 549 MPa (s.d. = 3 MPa) and ultimate strength of 698 MPa (s.d. = 4 MPa) whilst the 8 mm plain bars had yield strength of 385 MPa (s.d. = 1 MPa) and ultimate strength of 451 MPa (s.d. = 2 MPa).

2.3. Corrosion process

The accelerated corrosion process was induced by impressing a constant direct current of 150 mA on the tensile steel bars. It was limited to the tensile reinforcement and to a length of 700 mm at the centre of the beams by building a NaCl pond on the extreme tensile face of the beams to contaminate only the region to be corroded as shown in Figs. 1–3. Assuming the limitation of steel corrosion to the desired length, the applied current corresponded to a current density of 189 μA/cm^2. It is acknowledged that this current density is much larger than the current densities in real structures which normally range between 0.1 and 100 μA/cm^2 [20,24]. The intention of the accelerated corrosion test was to produce desired structural damage within a reasonable time frame but without excessively altering the structural response that would be obtained under natural steel corrosion. In the absence of a testing standard for accelerated corrosion of RC laboratory specimens, a guide from [23] that impressed current densities should be limited to 200 μA/cm^2 was followed. This is one area that still requires extensive research as well as standardisation.

The electrical connections to the power supply were such that the steel bars acted as the anode and a 12 mm stainless steel bar of length 250 mm, placed at the extreme tensile face of the beams acted as a cathode. The corrosion process involved cycles of four days wetting of the pond with a 5% solution of NaCl followed by two days drying of the pond under natural laboratory conditions. The total wetting days was limited to 44 days which according to Faraday's Law, is equivalent to a

Table 1
Experimental programme.

Beam	Sustained load as % of ultimate capacity	f′c, MPa (s.d.)	Crack pattern
1	1	50.8 (0.6)	Pattern B
2	1	46.6 (1.1)	Pattern B
3		38.9 (1.4)	Pattern B
4		38.9 (1.4)	Pattern B
5	8	35.2 (0.8)	Pattern B
6		40.1 (1.3)	Pattern B
7	12	44.0 (1.1)	Pattern B
8		44.0 (1.1)	Pattern B
9		40.1(1.3)	Pattern C
10	8[a]	40.1 (1.3)	Pattern B
11		40.1 (1.3)	Pattern A

[a] Beams under an extended testing programme.

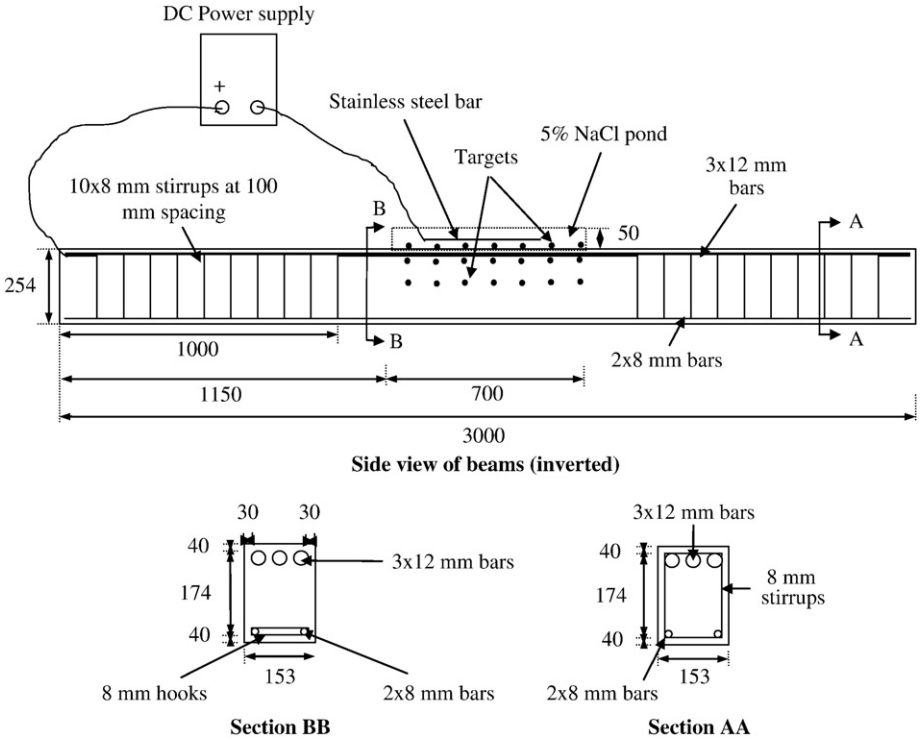

Fig. 3. Reinforcement configuration of test beams.

loss of area of steel of about 10%. Anodic current was only applied during the wetting period. The corrosion process used in this research is similar to the one described in [11,15,19].

2.4. Strain measurements

Lateral deformation of the RC beams due to steel corrosion was assessed by monitoring lateral strains applied on the concrete at various potential cracking regions. This is in contrast with the majority of previous works where lateral deformation on concrete due to expansive corrosion products was presented as corrosion crack widths that were directly measured using various devices such as magnification lenses, microscopes and crack compactors [3,6,12,13,22]. The advantages of using lateral strains over using crack widths to assess the behaviour of corroding RC specimens have also been seen elsewhere: [19,20] found the use of strain gauges to be very informative at the early corrosion stages when cracks were not visible; [25,26] found strain gauges to be useful after strengthening specimens by externally bonding them with fibre reinforced polymers when the cracks were covered; and probably most importantly to this research, [13] showed that if lateral strains are strategically monitored on cracking areas, they can easily be converted to corrosion crack widths.

In this programme, lateral strains were measured using a 100 mm demountable mechanical (demec) strain gauge with a range of ±10 to ±5000 micro strains. A minimum strain of 10 micro strains recorded from the gauge is therefore equivalent to a lateral expansion or a crack widening of 0.001 mm. Lateral strains were monitored at seven different locations along the beam to show not only how they vary with the level of corrosion, but also how they vary along the beam. For the first set of beams tested in the research programme, the experimental set-up was such that strains could only be measured at the extreme tensile face. For the subsequent set of beams, they were also measured on different potential cracking faces of the beams as described in detail in [19] and as shown in Figs. 3 and 4.

2.5. Measurements of the level of corrosion

Following the entire testing process (which included steel corrosion, flexural test of beams with exposed reinforcement, patch repair of beams whilst under a sustained load, strengthening of beams with externally bonded fibre reinforced polymers also whilst under a sustained load and the test of beams to failure), RC beams were broken and the corroded steel bars were retrieved. The bars in the concrete were cut at least 150 mm beyond each end of the corrosion region where there was no visual sign of corrosion. They were then cleaned of rust according to the ASTM G-1 standard [27].

For the first set of beams, steel bars were cut to coupons of about 100 mm in length. After noticing that there was a significant range in the mass loss of bars along the corrosion region, steel bars in subsequent beams were cut to coupons of about 50 mm in length. The coupons were then weighed and their actual length measured to determine their mass per length. The percentage gravimetric mass loss of a steel coupon, Q_{gi}, was calculated from Eq. (1).

$$Q_{gi} = \frac{\mu_u - \mu_i}{\mu_u} \cdot 100 \quad (1)$$

Where; μ_u is the average mass per length of an uncorroded steel coupon (=0.888 g/mm of length for the 12 mm bars used in the programme); and μ_i is the mass per length of a corroded coupon.

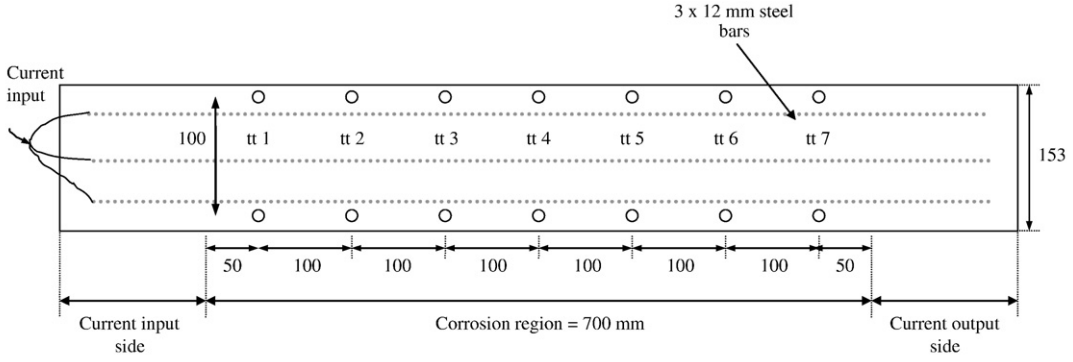

a) Location of targets for strain measurements on the extreme tensile face a beam (plan view of the beam)

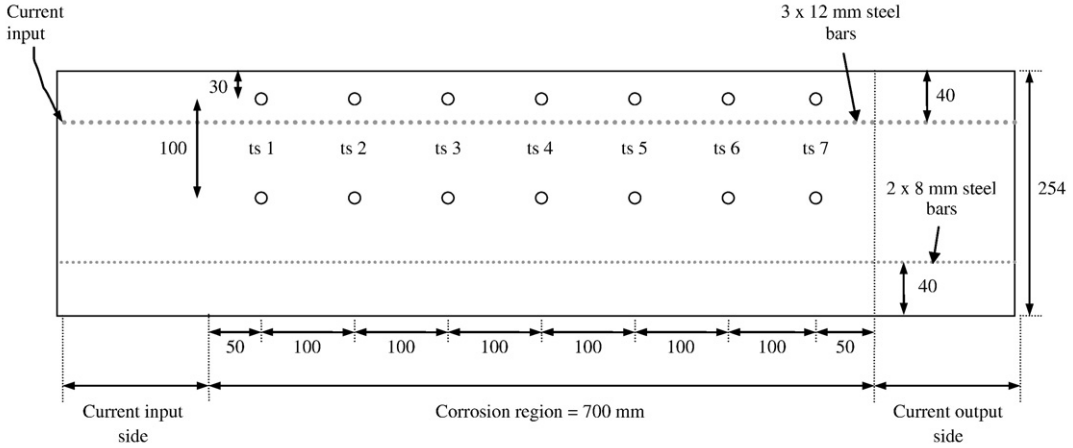

b) Location of targets for strain measurements on the side face of a beam (side view of the beam)

Fig. 4. Location of targets for strain measurements on beams.

This procedure of measuring mass loss of steel is different from procedures previously used by other researchers which measure the average gravimetric mass loss of the entire corroded steel bar [10,12,13,18,20] and the pit depth [3,22]. Its advantages over the previous methods is that: the average mass loss does not indicate the variation of mass loss of steel along the bar; the actual diameter of an uncorroded deformed bar often varies along the bar due to varying rib heights which makes it difficult to later relate the reduced bar diameters due to corrosion with the loss in area of steel bars; and loss in section of the steel due to corrosion is not uniform as was shown by [19,28].

3. Results

3.1. Corrosion crack patterns

During the corrosion process, RC beams in this programme exhibited three main types of corrosion crack patterns namely; crack pattern A, crack pattern B and crack pattern C. In crack pattern A, a single crack that propagated parallel to the corroded steel bars was observed on the extreme tensile face of the beam where corrosion agents were drawn into the concrete. Within the corrosion region, this crack was mostly at the centre of the beam. However, at a distance of about 50 mm before or beyond each end of the corrosion region, the crack split into two and the crack splits diverged to opposite side edges of the beam. The split cracks then crossed to the side faces and propagated to a distance of about 150 mm beyond the ends of the corrosion region and also parallel to the corroded bars as shown in Fig. 5a. The ends of the crack (now on the side face) coincided with the edges of the constant moment region. Only one beam (beam 11) from the eleven beams tested in the programme exhibited this crack pattern.

In crack pattern B, the beam initially cracked on its extreme tensile face as in crack pattern A. However, as the level of corrosion increased, another crack was observed on one side face of the beam whilst the other side face remained uncracked. The crack on the side face of the beam was at the level of the corroding tensile reinforcement and propagated (parallel to the bars) to a distance of about 150 mm beyond the ends of the corrosion region as shown in Fig. 5b. At a distance of about 50 mm beyond each end of the corrosion region, the crack on the extreme tensile face diverged to the side edge of the beam that belonged with the uncracked side face. In contrast to a crack in pattern A, the crack at the extreme tensile face for cracks in pattern B did not split into two and did not cross to the side face of the beam either. The majority of the beams tested (nine beams) exhibited this crack pattern. The times at which the crack patterns in various beams changed from crack pattern A to crack pattern B were however, uncommon and ranged from about 20 days to about 40 days.

In crack pattern C, the beam initially cracked on its extreme tensile face followed by a single crack on each side face as the level of corrosion progressed. In this pattern, the crack on the extreme tensile face ended in the middle of the face (at a distance of about 150 mm beyond the end of the corrosion region) and did not diverge to the side edges of the beam as in the other crack patterns. The cracks on the side faces were similar to the single crack on one side face in crack pattern B. Similar to crack pattern A, only one beam (beam 9) exhibited this crack pattern. It is important to mention that the cracks on the side faces in crack pattern C were observed at different times. For beam 9 they were observed after 25 days and after 45 days of testing.

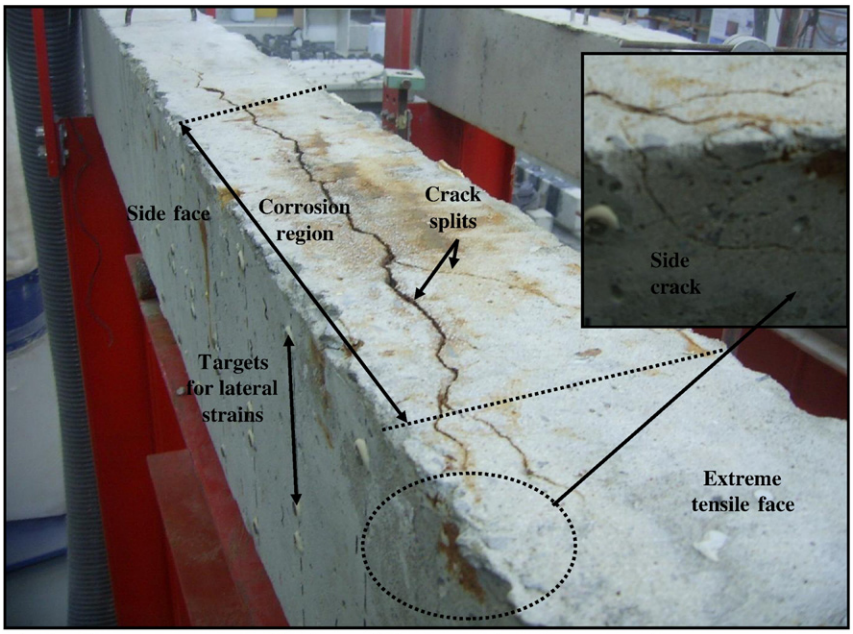

a) Crack on extreme tensile face of the beam (crack pattern A)

b) Crack on side face of the beam (crack pattern B or C)

Fig. 5. Corrosion crack patterns.

The above discussed crack patterns were the main crack patterns that were observed on the tested beams. In a few beams, side faces that were considered uncracked actually had small isolated corrosion cracks which probably indicated a change between crack patterns. It is acknowledged that similar crack patterns have also been reported elsewhere [13,16,20,29]. The difference between these crack patterns and crack patterns found by other researchers is that they at times found multiple cracks on the extreme tensile face that propagated along the positions of each reinforcing bar. This is probably because they used larger spacing between the bars. For example, [13] had a spacing of about 70 mm between bars whilst in this programme a spacing of 18 mm between bars was used. Both spaces between bars are practical and accepted in various design codes such as [31]. It was found in this programme and also by other researchers [13,16,29] that even for identical specimens, it is difficult to predict the type of crack pattern that each specimen will exhibit. However, the majority of specimens in this programme and elsewhere [13,16,29] exhibited crack pattern A at the early corrosion stages which then changed to crack pattern B as the level of steel corrosion increased. The relations between the various crack patterns and the rate of widening of each crack, which are the more important concerns are however, uncertain. This is most likely because the previous researchers either measured crack widths at one location along the specimens during the corrosion process or they meticulously measured crack widths at the end of the test.

3.2. Relation between crack patterns and the rate of widening of cracks

The lateral strains and hence crack widths, induced by the expansive corrosion products on the various faces of the beams were, as expected, closely related to the corrosion crack patterns. In a beam that exhibited corrosion crack pattern A, the majority of lateral strains recorded on uncracked side faces of the beam were compressive whilst, as expected, lateral tensile strains were recorded on the cracked extreme tensile face of the beam as shown in Fig. 6a. The figure also shows that each measuring point along the tensile face of the beam demonstrated a near-constant rate of increase of lateral tensile strains during the indicated time of testing. This implies that the width of cracks at the extreme tensile face widened with the level of corrosion and at a near-constant rate.

For a beam that exhibited crack pattern B, lateral tensile strains were experienced on the faces of the beam that had corrosion cracks whilst compressive strains were recorded on the uncracked side face. Before the appearance of the crack on the side face, the rate of increase of lateral tensile strains on the extreme tensile face of the beam was nearly constant and about the same as in crack pattern A. Interestingly, following the appearance of the crack on the side face (25 days for beam 10), the rate of increase of the corresponding lateral tensile strains on the extreme tensile face decreased whereas the rate of increase of the lateral tensile strains on the (now) cracked side face of the beam was nearly constant through the entire testing process as shown in Fig. 6b.

Lateral strains found in crack pattern C were initially similar to those measured in crack pattern A followed by those in crack pattern B. In contrast to crack patterns A and B, when both sides of the beam cracked in crack pattern C (45 days for beam 9), the lateral tensile strains at the extreme tensile face of the beam seized to increase despite a continued increase in the level of corrosion. The rate of increase of lateral tensile strains on the side faces of the beam however, remained positive and near constant through the entire testing process as shown in Fig. 6c. Interestingly, and essential to understanding the relation between corrosion crack widths and the various corrosion crack patterns, the rate of widening of corrosion cracks on the side faces of beams in crack patterns B and C was almost the same as the rate of widening of corrosion cracks at the extreme tensile face of a beam with crack pattern B ($\approx$0.009 mm/day).

It is evident that compared to beams that exhibit crack pattern A (where there was always a near-constant rate of widening of corrosion cracks), corrosion cracks in beams that have crack pattern B will have a lesser width whilst beams that exhibit crack pattern C will have the narrowest corrosion cracks. As previously mentioned, prior to the change of crack patterns the beams exhibited about the same rate of widening of corrosion cracks. For example, Fig. 6 clearly shows that after 20 days of accelerated corrosion testing (when the beams had crack pattern A), crack widths in each of the beams 9, 10 and 11 ranged from 0.2 mm to 0.4 mm. This range of corrosion crack widths covers the lower limit corrosion crack width of 0.3 mm that the DuraCrete Final Technical Report [30] uses as a criterion for the end of service life of corrosion-affected RC structures. This indicates that the service life of corrosion-affected structures on the basis of a crack width of 0.3 mm is not significantly variable between identical structures. After 65 days of corrosion however, beam 11 (still with crack pattern A) had a maximum crack width of 1 mm whilst beam 9 (now with crack pattern C) had a maximum crack width below 0.6 mm at the extreme tensile face. Moreover, the maximum crack width of 0.6 mm at the extreme tensile face in beam 9 was dormant whilst the actively widening crack on the side face of the beam had a crack width of about 0.2 mm. In contrast, the crack width of 1 mm in beam 11 was still actively widening. The obvious implication is that end of service life that is based on the criterion of maximum corrosion crack width of 1 mm is likely to suggest reinstatement of RC structures with crack pattern A prior to reinstatement of structures with crack pattern C. Similar to crack pattern A, results from [16] on beams that were corroded under natural steel corrosion for an excess of 23 years suggest that when a crack on the extreme tensile face is actively widening, the rate of widening of an adjacent crack on the side face of the beam is relatively low. One important research element that is still unclear however, is how these crack patterns relate to the level of steel loss and subsequently, to the residual capacity of the structures.

To later enable an easier relation of maximum corrosion crack widths with the level of steel corrosion, Fig. 7 shows the variation of lateral tensile strains along the corrosion region (at the extreme tensile face) for the various beams tested in the programme. The position along the beam shown in the figure was measured from the current input side of the beam to the current output side. Zero in the figure therefore indicates the edge of the corrosion region on the current input side whilst 700 mm indicates the edge of the region on the current output side. In each crack pattern, the lateral strains on the extreme tensile face varied along the corroded region with the maximum strains experienced at the centre of the corrosion region and very low strains were experienced at the ends of the region. Only lateral tensile strains at the extreme tensile face are shown in the figure because for all beams in this programme, maximum crack widths were at the extreme tensile face of the beams. This was true despite cracks at the extreme tensile face in beam 9 having been dormant for nearly half the total time of testing. If steel corrosion was to be continued, it is expected however, that the maximum crack widths in beam 9 would belong with the side face as opposed to the extreme tensile face.

Even though the general behaviour of the lateral tensile strains along the corrosion region was the same for all beams shown in Fig. 7, the magnitude of the strains was different for each beam. Owing to the varying times at which different corrosion crack patterns were observed on the beams and that the rate of widening of the cracks was closely related to the crack patterns, the beams were expected to show varying corrosion crack widths. As discussed earlier, the figure clearly shows that the beam with crack pattern A had much wider cracks and the narrowest cracks belonged with a beam with crack pattern C. Considering the large variation between the dominant lateral tensile strains for the various beams displayed in Fig. 7 (even for beams with the same crack patterns) and that the beams exhibited a similar shape of lateral strains along the corrosion region, it is logical to present the strains as an envelope rather than an average. The

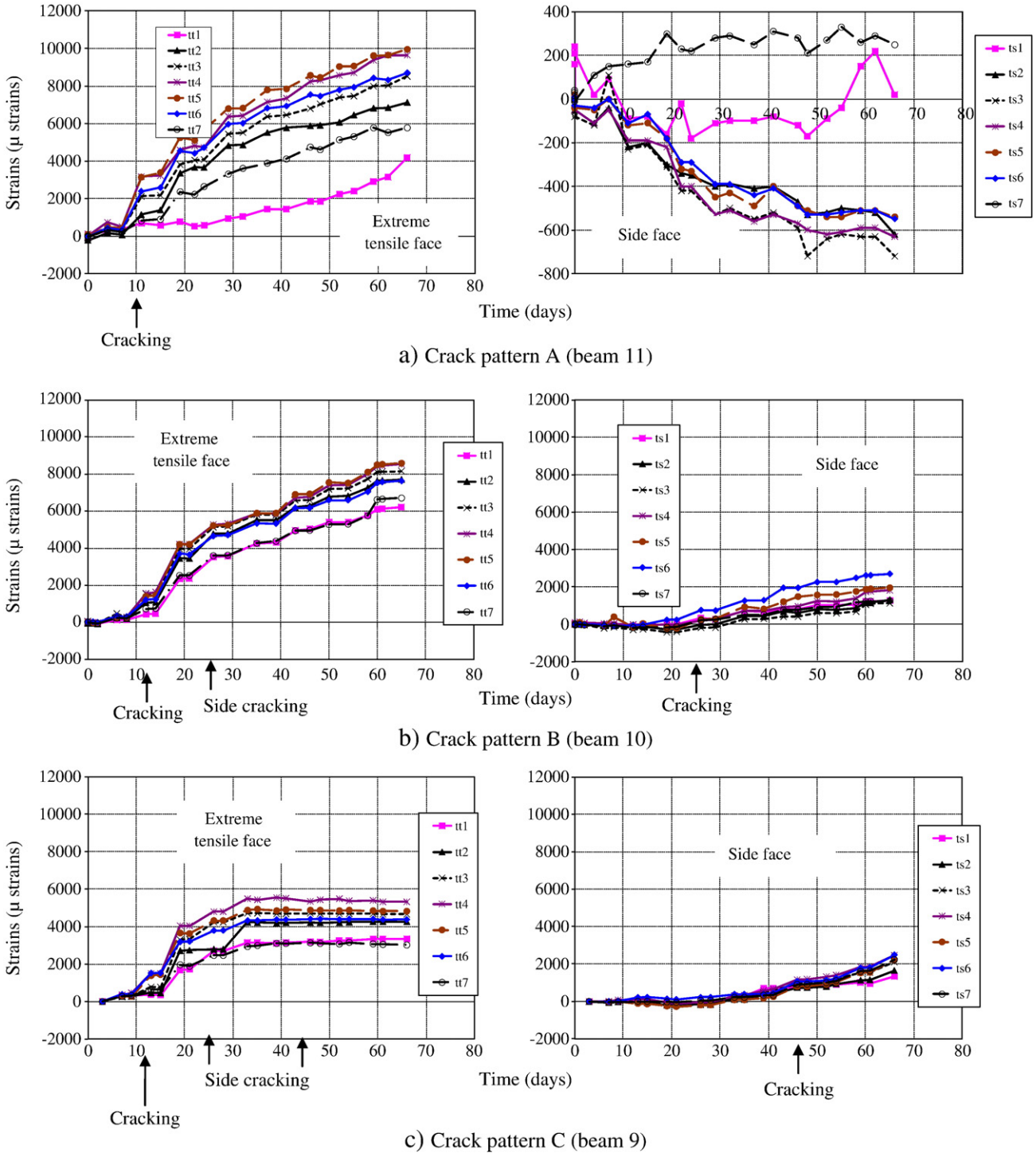

Fig. 6. Lateral strains in various crack patterns.

lower and upper bounds of the envelope can be represented by the following trend-lines;

$$\text{Lower bound strains (micro strains)} = -0.04x^2 + 25.3x + 710.8 \quad R^2 = 0.97 \tag{2}$$

$$\text{Upper bound strains (micro strains)} = -0.04x^2 + 28.4x + 4815.3 \quad R^2 = 0.98. \tag{3}$$

In agreement with previous work by [19], the figure shows that the strains were independent of both the strength of the concrete as well as the level of the sustained load. This is probably because the corrosion process used in the test was accelerated to a rate that is much larger than the natural rate of corrosion of in-service structures [20,24]. Further work is ongoing to assess the effect of the level of the sustained load on the rate of deformation of beams under natural corrosion.

3.3. Variation of steel loss along the beam

The average percentage mass loss of steel for every measured section (50–100 mm) along the corroded length was calculated as the average percentage mass loss of the three steel coupons corresponding to that

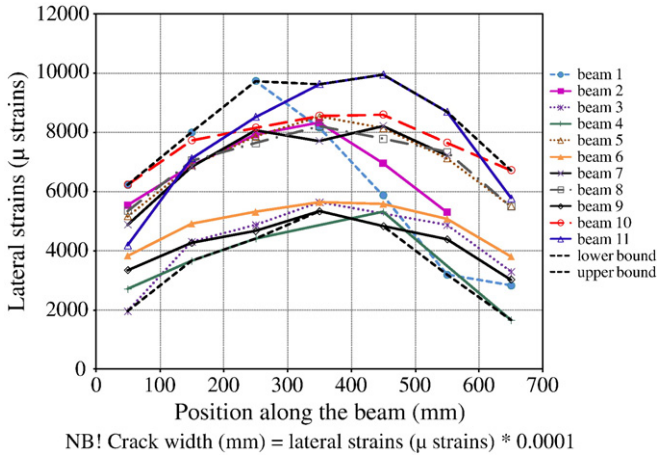

Fig. 7. Variation of lateral tensile strains along the corrosion region at the end of the test.

section and its variation along the beam is shown in Fig. 8. From this figure, it is clear to observe that the general variations of mass loss of bars along the corrosion region behaved like a parabola with a maximum vertex close to the centre of the corrosion region. The loss of steel extended to about 150 mm beyond the ends of the corrosion region, which agrees well with the ends of the corrosion cracks. It is also evident from the figure that the level of mass loss of steel and its variation along the beam were independent of the level of the sustained load and probably most importantly, were independent of the pattern of corrosion cracks. Similar to the variations of dominant lateral tensile strains of the beams along the corrosion region (Fig. 7), mass loss of steel in different beams was distributed similarly along the corrosion region but at different scales. The variation of mass loss of steel in different beams was therefore also presented as an envelope that had the boundaries with the following trend-lines;

$$\textit{Lower bound mass loss of steel}\,(\%) = -3E{-}05x^2 + 0.017x + 3.36 \quad R^2 = 0.81 \tag{4}$$

$$\textit{Upper bound mass loss of steel}\,(\%) = -5E{-}05x^2 + 0.035x + 10.25 \quad R^2 = 0.97. \tag{5}$$

It is important to note that the maximum mass loss of steel for each beam was larger than the mass loss predicted from Faraday's Law

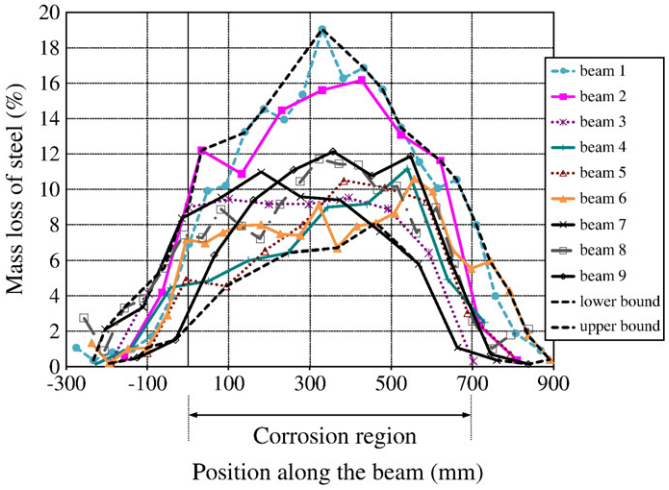

Fig. 8. Variation of mass loss of steel along the beam.

(10%). The ratio between the measured maximum mass losses of steel to the mass loss from Faraday's Law ranged from 1.2 to 1.9. Around the ends of the corrosion region however, steel loss from Faraday's Law was larger than the measured mass loss of the steel. This might be the reason why researchers who measured overall mass loss of steel found Faraday's Law to under-predict it at low levels of corrosion (<5%) and to over-predict it at high levels of corrosion (>10%) [23,25]. The implication is that properties of RC structures that rely on the maximum loss of steel such as the flexural capacity are likely to be underestimated by the level of steel corrosion that is predicted from Faraday's Law. The interests of this paper are on the relation between corrosion crack widths and the maximum mass loss of steel.

4. Discussion of results

The relation between the envelope of the dominant lateral tensile strains and the envelope of the mass loss of steel along the corrosion region and at the end of the corrosion process is shown in Fig. 9. It is important to recall from Fig. 7 that the lower bound lateral strains belonged with beams with crack pattern C whilst the upper bound belonged with a beam with crack pattern A. Fig. 8 however showed that there was no conclusive relation between the mass loss of steel and corrosion crack patterns. This suggests that a beam that exhibits crack pattern C, even though having narrower corrosion crack widths than a beam that exhibits crack pattern A, can have larger levels of steel corrosion and vice-versa.

Figs. 7–9 therefore imply that a beam that exhibits crack pattern C and has a maximum crack width of 0.6 mm may have a maximum mass loss of steel varying from about 8% to about 19%. The similar range of maximum mass loss of steel of 8% to 19% however, corresponds to a maximum crack width of 1 mm if a beam exhibits crack pattern A. As previously mentioned, a corrosion crack width of 1 mm is specified by [30] as the most severe serviceability state using the criterion of corrosion crack widths. Clearly, to structural engineers and asset managers who are mainly concerned with the residual capacity of structures because of the severe consequences of collapse, the worst case scenario is when a beam exhibits crack pattern C and has the largest rate of mass loss of steel. From Fig. 6 and assuming the current rate of widening of cracks and that no spalling of the cover concrete occurs, it is evident that a crack width of 1 mm on beam 9 was most probably going to be observed on the side face of the beam after about 170 days of accelerated steel corrosion. If the beam had the maximum recorded rate of loss of steel in this programme (19% mass loss of steel after 65 days), then at the time of reinstatement on the basis of the guidelines from [30], the beam was expected to have a mass loss of steel of about 50%. Furthermore, the principal assumption in analytical models to relate the width of corrosion cracks with the level of steel corrosion is that there is either one crack or if there are multiple cracks then they have equal widths [7,8]. From the results in this programme, this assumption applies to crack pattern A. This shows that despite the complexity of the analytical models, they are not applicable to crack pattern C which reiterates the earlier notion that crack pattern C offers the worst case scenario.

The large range of mass loss of steel necessary to reach a critical corrosion crack width that indicates the end of service life clearly shows that service life of corrosion-affected RC structures on the basis of corrosion crack widths should not only consider the maximum crack width, but also the pattern of corrosion cracks. As discussed earlier, Fig. 6 shows that the rates of widening of cracks on the side faces of beams with crack patterns B and C were about the same as the rate of widening of cracks at the extreme tensile face in crack pattern B (≈0.009 mm/day). Since the majority of the beams in this programme exhibited crack pattern B, it is recommended that if a corrosion-affected RC structure exhibits crack pattern C, then the maximum crack width on the structure should be taken as the sum of

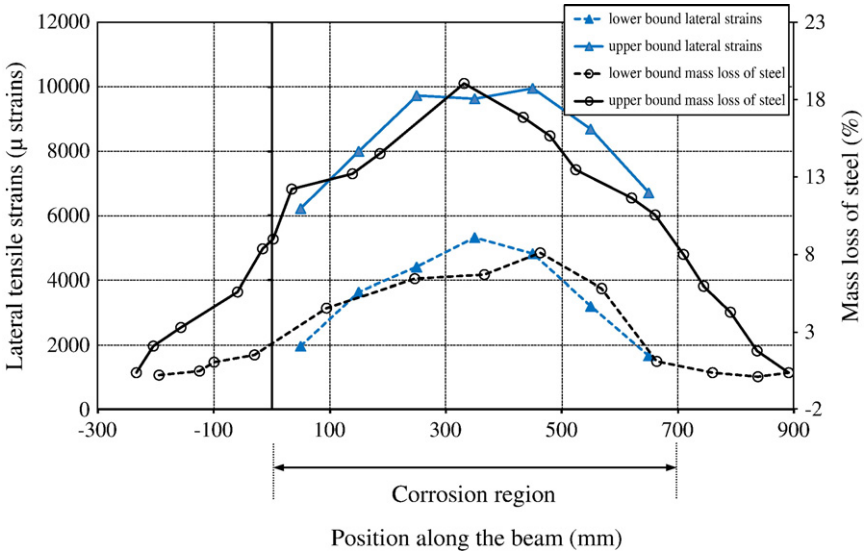

Fig. 9. Relation between mass loss of steel and lateral tensile strains.

the maximum crack width at the extreme tensile face and the maximum crack width on the near side face. From the results in this programme, this gives beam 9 (crack pattern C) a maximum crack width of 0.8 mm which is comparable with the maximum crack width found in beam 10 (crack pattern B).

5. Conclusions

It was shown in this programme that a corrosion crack width of 0.3 mm which is one of the criteria for end of service life of corroding RC structures [30] was observed at about the same time for various beams used in the programme. If however, a corrosion crack width of 1 mm was to be used as a criterion for end of service life then similar beams were found to have significantly varying times for end of service life depending on their pattern of corrosion cracks. The rate of loss of steel was however found not to be dependent on the crack patterns. It was shown that to reach a crack width of 1 mm, the beams were likely to have mass losses of steel ranging from 8% to 50%. It was therefore recommended that for beams that exhibit cracks on the extreme tensile face as well as on the near side face, the maximum crack width should be taken as the sum of the maximum cracks for each face of the beam. If the recommendations in this programme are followed then a maximum crack width of 0.8 mm is reached at a mass loss of steel ranging from 8% to 19%. To be conservative, a mass loss of steel of 1% corresponds to a maximum corrosion crack width of 0.04 mm.

Other researchers have found that a mass loss of steel of 1% generates a maximum crack width of 0.08 mm [20] whilst others [3] found a mass loss steel of 1% to induce crack widths of around 0.03 mm. These results are similar to those obtained in this programme for crack pattern B. The principal difference between this programme and the previous programmes is that in this programme it is clearly shown using the rate of widening of corrosion cracks in different crack patterns that using the relations between mass loss of steel and corrosion crack widths without understanding the rates of widening of corrosion cracks may result in some structures being repaired at unbearable levels of steel corrosion. For example, relation between mass loss of steel and crack widths from [3] suggests that a crack width of 1 mm will be obtained at a mass loss of steel of 12.5%. This agrees with results for crack patterns A and B in the programme. If 12.5% represents a critical level of steel corrosion necessary for reinstatement of structures, according to this relation, a crack width below 1 mm indicates that the level of steel corrosion is below critical. It was however shown in the programme that under crack pattern C, a beam may reach a crack of 1 mm after a mass loss of steel of 50%.

Acknowledgements

The support of the University of Botswana and the Concrete Materials & Structural Integrity Research Group (CSIRG) at the University of Cape Town is greatly acknowledged.

References

[1] P.R. Roberge, Handbook of Corrosion Engineering, McGraw-Hill, New York, 1999.
[2] Federation International du B'eton — FIP Bulletin. Bond of reinforcement in concrete, state-of-the art report. Bulletin No. 10. International Federation for structural concrete, Switzerland, 2000.
[3] A.A. Torres-Acosta, S. Navarro-Gutierrez, J. Terán-Guillén, Residual flexure capacity of corroded reinforced concrete beams, Engineering structures vol 29 (2007) 1145–1152.
[4] X. Wang, X. Liu, Bond strength modelling for corroded reinforcements, Construction and building materials 20 (2006) 177–186.
[5] L. Berto, P. Simioni, A. Saetta, Numerical modelling of bond behaviour in RC structures affected by reinforcement corrosion, Engineering Structures 30 (2008) 1375–1385.
[6] T. Vidal, A. Castel, R. Francois, Analyzing crack width to predict corrosion in reinforced concrete, Cement and concrete research 34 (2004) 165–174.
[7] C. Li, R.E. Melchers, J. Zheng, Analytical model for corrosion-induced crack width in reinforced concrete structures, ACI Structural Journal 103 (2006) 479–487.
[8] C. Li, J. Zheng, W. Lawanwisut, R.E. Melchers, Concrete delamination caused by steel reinforcement corrosion, Journal of Materials in Civil Engineering 19 (2007) 591–600.
[9] T. El Maaddawy, K. Soudki, T. Topper, Analytical model to predict nonlinear flexural behaviour of corroded reinforced concrete beams, ACI structural journal 102 (4) (2005) 550–559.
[10] A.K. Azad, S. Ahmad, S.A. Azher, Residual strength of corrosion-damaged reinforced concrete beams, ACI materials journal 104 (1) (2007) 40–47.
[11] G. Malumbela, M. Alexander, P. Moyo, Steel corrosion on rc structures under sustained service loads — a critical review, Engineering Structures 31 (2009) (2009) 2518–2525.
[12] Y. Ballim, J.C. Reid, Reinforcement corrosion and deflection of RC beams—an experimental critique of current test methods, Cement and concrete composites 25 (2003) 625–632.
[13] T. El Maaddawy, K. Soudki, T. Topper, Long-term performance of corrosion-damaged reinforced concrete beams, ACI Structural Journal 102 (2005) 649–656.
[14] S. Yoon, K. Wang, J. Weiss, S. Shah, Interaction between loading, corrosion, and serviceability of reinforced concrete, ACI materials journal 97 (6) (Nov–Dec 2000) 637–644.
[15] G. Malumbela, P. Moyo, M. Alexander, Behaviour of RC beams corroded under sustained service loads, Construction and Building Materials 23 (11) (2009) 3346–3351.
[16] R. Zhang, A. Castel, R. François, Serviceability limit state criteria based on steel–concrete bond loss for corroded reinforced concrete in chloride environment, Materials and structures (2008), doi:10.1617/s11527-008-9460-0.
[17] A.A. Almusallam, A.S. Al-Gahtani, A.F. Aziz, Rasheeduzzafar, Effect of reinforcement corrosion on bond strength, Construction and building materials 10 (2) (1996) 123–129.
[18] J. Cairns, Y. Dut, D. Law, Structural performance of corrosion-damaged concrete beams, Magazine of Concrete Research 60 (5) (2008) 359–370.

[19] G. Malumbela, M. Alexander, P. Moyo, Lateral deformation of RC beams under simultaneous load and steel corrosion, Construction and Building Materials 24 (2010) 17–24.
[20] C. Alonso, C. Andrade, J. Rodriguez, J.M. Diez, Factors controlling cracking of concrete affected by reinforcement corrosion, Materials and structures 31 (1998) 435–441.
[21] K. Bhargava, A.K. Ghosh, Y. Mori, S. Ramanujam, Analytical model for time to cover cracking in RC structures due to rebar corrosion, Nuclear Engineering and Design 236 (2006) 1123–1139.
[22] A.A. Torres-Acosta, M.J. Fabela-Gallegos, A. Munoz-Noval, D. Vazquez-Vega, T.R. Hernandez-Jimenez, M. Martinez-Madrid, Influence of corrosion on the structural performance of reinforced concrete beams, Corrosion 60 (2004) 862–872.
[23] T. El Maaddaway, K. Soudki, Effectiveness of impressed current technique to simulate corrosion of steel reinforcement in concrete, Journal of materials in civil engineering 15 (1) (2003) 41–47.
[24] C. Andrade, C. Alonso, On-site measurements of corrosion rate of reinforcements, Construction and building materials 15 (2001) 141–145.
[25] M. Badawi, K. Soudki, Control of corrosion-induced damage in reinforced concrete beams using carbon fiber-reinforced polymer laminates, Journal of composites for construction 9 (2) (2005) 195–201.
[26] K. Soudki, T.G. Sherwood, Behaviour of reinforced concrete beams strengthened with carbon fibre reinforced polymer laminates subjected to corrosion damage, Canadian journal of civil engineering 27 (2000) 1005–1010.
[27] ASTM G1-03, Standard practice for preparing, cleaning, and evaluating corrosion test specimens, Annual book of ASTM Standards 03-02 (2003) 17–26.
[28] Y. Yuan, Y. Ji, Modeling corroded section configuration of steel bar in concrete structure, Construction and building materials 23 (6) (2009) 2461–2466.
[29] A.A. Torres-Acosta, A.A. Sag¨u´es, Concrete cracking by localized steel corrosion—geometric effects, Mater J 1 (6) (2004) 501–507.
[30] DuraCrete. The European Union-Brite EuRam III, DuraCrete final technical report, Document BE95-1347/R17. 2000.
[31] South African National Standards Structural Use of Concrete—Part 1: Design (SANS 10100-1:1992). 1992. Pretoria: The Bureau.